Contrasting low-mode noise reduction techniques for light HISQ meson propagators

Michael T. Lynch [1] Carleton DeTar [2]

[1]University of Illinois, Urbana-Champaign, Urbana, IL, USA [2]University of Utah, Salt Lake City, Utah, USA

Introduction

Long-distance correlations are often dominated by the lowest eigenmodes (low modes) of the Dirac operator. Reducing the long-distance noise is key to meeting precision goals for observables such as the HVP contribution to the anomalous magnetic moment of the muon. We compare three methods for noise reduction.

All results were generated using the MILC collaboration's Highly Improved Staggered Quark (HISQ) ensembles and with code modified from the Hadrons and Grid C++ libraries.

Methods

Method 1. Random Wall (RW)

This traditional method introduces N_r random ($\mathbb{Z}^2$) sources on each of N_s time slices t_j, denoted by $\eta_i(\mathbf{x}, t_j)$, calculates the hadronic correlation function from each time slice, and averages over source times and random sources: The quark field at the sink is

$$S_{\mathrm{RW},i}(\mathbf{x}, t; t_j) = \sum_{\mathbf{y}} M^{-1}(\mathbf{x}, t; \mathbf{y}, t_j)\eta_i(\mathbf{y}, t_j).$$

The hadronic correlation function is

$$C^{\Gamma}_{\mathrm{RW}}(\delta t) = \frac{1}{N_r N_s}\sum_{i=1}^{N_r}\sum_{j=1}^{N_s}\sum_{\mathbf{x}} tr\left[S_{\mathrm{RW},i}(\mathbf{x}, \delta t + t_j; t_j)\Gamma\gamma_5 S^{\dagger}_{\mathrm{RW},i}(\mathbf{x}, \delta t + t_j; t_j)\gamma_5\Gamma\right].$$

Method 2. All-to-all (A2A) [1]

We work with N_e low eigenmodes with eigenvectors v_i and N_r random wall sources $\eta_{i,j}(\mathbf{x}) \equiv \eta_i(\mathbf{x}, t_j)$ on *all* N_t time slices with low modes removed:

$$\mathbb{P}\eta_{i,j} = \left(\mathbb{I} - \sum_{k=1}^{N_e} v_k v_k^{\dagger}\right)\eta_{i,j}.$$

We construct "meson fields" $\mathcal{M}^{\Gamma}_{i,j}(t)$,

$$\mathcal{M}^{\Gamma}_{i,j}(t) \equiv \sum_{\mathbf{x}} w_i^{\dagger}(\mathbf{x}, t)\Gamma u_j(\mathbf{x}, t)\,,$$

where

$$w_i \in \{v_1/\lambda_1, \ldots, v_{N_e}/\lambda_{N_e}, \psi_{1,1}\ldots, \psi_{N_r,N_t}\}\,,$$
$$u_i \in \{v_1, \ldots, v_{N_e}, \mathbb{P}\eta_{1,1}, \ldots, \mathbb{P}\eta_{N_r,N_t}\}$$

with $\psi_{i,j}(\mathbf{x}, t) = S_{\mathrm{RW},i}(\mathbf{x}, t; t_j)$. The correlation function is then,

$$C^{\Gamma}_{A2A}(\delta t) = \frac{1}{N_t}\sum_{t}\sum_{i,j}\mathcal{M}^{\Gamma}_{i,j}(t)\mathcal{M}^{\Gamma}_{j,i}(t + \delta t)\,.$$

In Figure 1 (bottom right pane), we decompose C^{Γ}_{A2A} according to the N_e low eigenmodes (L) and the $N_s N_t$ stochastic high modes (H),

$$C^{\Gamma}_{\mathrm{A2A}} = C^{\Gamma}_{\mathrm{A2A,LL}} + C^{\Gamma}_{\mathrm{A2A,HL}} + C^{\Gamma}_{\mathrm{A2A,LH}} + C^{\Gamma}_{\mathrm{A2A,HH}}, \qquad (1)$$

and examine the relative statistical errors of each.

Method 3. Low-Mode–Improved Random Wall (RW+LMI) [2]

This method combines the low-mode improvement of DeGrand and Schaefer [3; 4] with the random wall Method 1. We separate the low- and high-mode contributions to the propagator $S_{\mathrm{RW}} = S_{\mathrm{RW,L}} + S_{\mathrm{RW,H}}$, where $S_{\mathrm{RW,H}}$ is

$$S_{\mathrm{RW,H},i}(\mathbf{x}, t; t_j) = \sum_{\mathbf{y}} M^{-1}(\mathbf{x}, t; \mathbf{y}, t_j)\mathbb{P}\eta_i(\mathbf{y}, t_j).$$

The full correlation function decomposes into low and high terms as in Eq. (1) where

$$C^{\Gamma}_{\mathrm{RW,JK}}(\delta t) = \frac{1}{N_r N_s}\sum_{i=1}^{N_r}\sum_{j=1}^{N_s}\sum_{\mathbf{x}} tr\left[S_{\mathrm{RW,J},i}(\mathbf{x}, \delta t + t_j; t_j)\Gamma\gamma_5 S^{\dagger}_{\mathrm{RW,K},i}(\mathbf{x}, \delta t + t_j; t_j)\gamma_5\Gamma\right].$$

We then replace the $C^{\Gamma}_{\mathrm{RW,LL}}(\delta t)$ contribution with the exact low-mode all-to-all result (no random sources) $C^{\Gamma}_{\mathrm{A2A,LL}}(\delta t)$:

$$C^{\Gamma}_{\mathrm{RW+LMI}}(\delta t) = C^{\Gamma}_{\mathrm{RW}}(\delta t) - C^{\Gamma}_{\mathrm{RW,LL}}(\delta t) + C^{\Gamma}_{\mathrm{A2A,LL}}(\delta t). \qquad (2)$$

The effect on the variance from this low-mode subtraction and replacement is displayed in Figure 1 (top right pane).

Results

Vector Current Noise Comparison

We compare all three methods on 64 configurations at $a \approx 0.12$ fm physical mass ($48^3 \times 64$). For each method we perform 768 CG solves and compute the lowest 2,000 low-mode pairs of the Dirac Matrix.

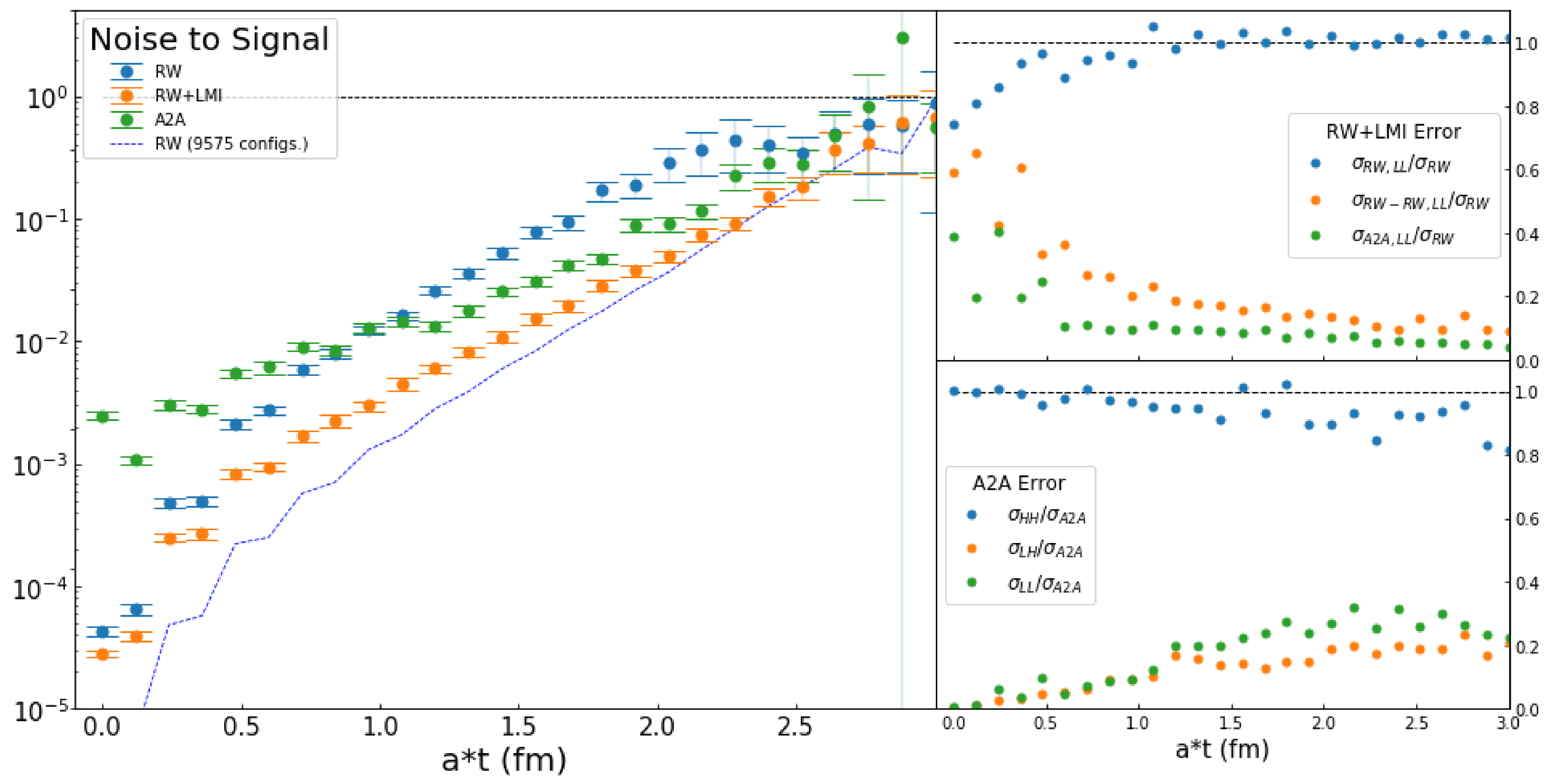

Figure 1. Noise to signal comparison of RW,RW+LMI, and A2A. RW+LMI offers best results at all time separations (left). Dominant contribution to RW error, C_{LMA}, is removed from RW+LMI (top right). Error of A2A components dominated by C_{LL} (bottom right)

RW+LMI Results at 0.06 fm

We repeat our analysis of the RW+LMI method on 30 configurations at $a \approx 0.06$ fm physical mass ($96^3 \times 192$), where we compute 288 CG solves and 2,000 low-mode pairs.

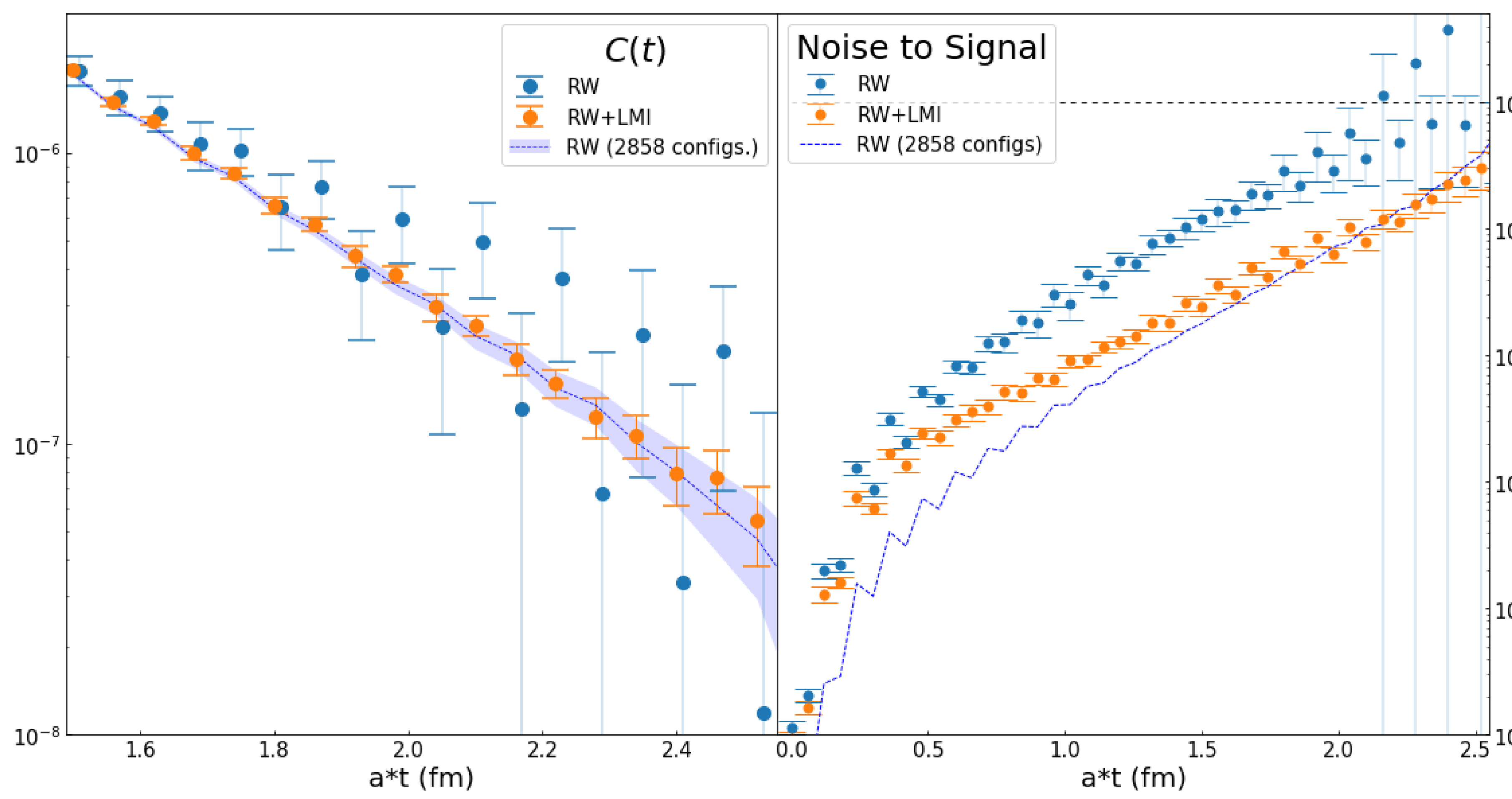

Figure 2. Light vector meson correlator at long-distance (left), and noise to signal comparison (right). Long-distance RW+LMI results (30 configs.) approach RW (2858 config.) results.

Remarks

While the all-to-all method suffers from large noise at short distances, the RW+LMI method offers superior results at all time separations, reducing the random wall error by over 80% in the region from 1.5-2.5 fm.

Including the cost of computing the eigenvectors, the RW+LMI method is more than double the cost of traditional random wall. In future work we plan to combine this method with truncated solves as in [5; 6] to further reduce cost.

References

[1] Foley J *et al.* 2005 *Computer Physics Communications* **172** 145–162
[2] Li A *et al.* 2010 *Phys. Rev. D* **82**(11) 114501
[3] DeGrand T and Schaefer S 2004 *Computer Physics Communications* **159** 185–191
[4] Aubin C *et al.* 2020 *Phys. Rev. D* **101**(1) 014503
[5] Shintani E *et al.* 2015 *Phys. Rev. D* **91**(11) 114511
[6] Bali G S *et al.* 2010 *Computer Physics Communications* **181** 1570–1583